Sustainable Energy Technologies and Assessments 91 (2026) 105052

Contents lists available at ScienceDirect

Sustainable Energy Technologies and Assessments

journal homepage: www.elsevier.com/locate/seta

Original article

Parametric bottom-up cost modelling of tidal energy converters for site-specific feasibility studies

M. Petri, E. Gorr-Pozzi *, M. Corrales-González, G. Giorgi

Marine Offshore Renewable Energy Lab (MOREnergy Lab), Department of Mechanical and Aerospace Engineering (DIMEAS), Politecnico di Torino, Corso Duca degli Abruzzi 24, 10129 Turin, Italy

ARTICLE INFO

Keywords:
Marine renewable energy
Tidal energy
Levelised cost of energy
Cost reduction
Electricity market
Bottom-up approach

ABSTRACT

Tidal energy represents a promising yet underexploited source within the marine renewable sector, offering predictable and sustainable generation potential that aims to increase interest in offshore energy alternatives. This study presents a detailed bottom-up techno-economic optimisation assessment model adapted to tidal energy converter (TEC) systems. The proposed novel methodology breaks down component-level costs for TECs into three foundational types: Gravity-Based Substructures (GBS), floating platforms, and monopiles. A key achievement of this work lies in departing from traditional macroscopic economic aggregates by dynamically coupling these structural requirements with local hydrodynamic and bathymetric data to evaluate energy yield and economic performance. The model is applied to five different locations, namely Fall of Warness (UK), Fromveur and Raz Blanchard (France), Punta Pezzo (Italy), and Cozumel (Mexico), to assess how local parameters affect the feasibility of the TEC plant. Validation against real-world data from the ATIR floating platform project shows strong agreement with actual deployment costs. Supported by a multi-variable sensitivity analysis, results from the case studies indicate that monopile and floating TECs typically achieve higher capacity factors and lower Levelised Costs of Energy (LCoE) compared to GBS systems. The monopile configuration is more suitable for shallow water, while floating platforms prove more cost-effective in deep-water sites. By highlighting the importance of tailoring TEC configurations to specific site conditions, these insights provide a robust and scalable tool for informing early-stage design and policy-making.

Introduction

Increasing pressure to reduce fossil fuel consumption and mitigate climate change has accelerated the expansion of renewable energy systems [1]. However, land availability and conflicts with agriculture and urban development limit further onshore deployment, increasing costs in land acquisition. Offshore renewable technologies offer a promising alternative due to the vast extent of marine areas, higher and more stable wind and current resources, and reduced visual impact [2]. Among them, tidal energy provides additional benefits such as high predictability, limited surface footprint, and consistent energy production [3,4].

Despite their potential, Marine Renewable Energy (MRE) technologies, such as Tidal Energy Converter (TEC) and Wave Energy Converter (WEC), remain at early deployment stages [5]. Their commercialisation is hindered by low learning rates, limited operational experience [6], and the scarcity of detailed techno-economic data. To overcome these commercialisation barriers, recent literature strongly emphasises the need for comprehensive techno-economic assessments. Recent investigations on hydrokinetic farms have highlighted how specific design parameters, such as turbine layout, capital expenditures (CapEx), and fluctuations in electricity prices, directly dictate key financial indicators like the LCoE and Net Present Value (NPV) [7]. However, while the importance of these parameters is well-established, linking them to specific foundation technologies remains a challenge. Existing cost models often rely on the Top-down Approach (TdA), which allocates total project cost across high-level components [5], offering limited flexibility in assessing alternative device configurations. The Bottom-up Approach (BuA) estimates the cost of each subcomponent, enabling more detailed and scalable evaluations. However, its application to tidal technologies is still limited. To date, only one BuA model exists [8], but it lacks sufficient detail and adaptability for practical use. The present work addresses this gap by developing comprehensive parametric BuA cost functions for TEC systems.

Tidal currents arise from periodic water level variations influenced by bathymetry and coastal geometry, with stronger flows in constrained

* Corresponding author.
E-mail addresses: petri.mattia00@gmail.com (M. Petri), emiliano.gorr@polito.it (E. Gorr-Pozzi), manuel.corrales@polito.it (M. Corrales-González), giuseppe.giorgi@polito.it (G. Giorgi).

https://doi.org/10.1016/j.seta.2026.105052
Received 21 November 2025; Received in revised form 3 April 2026; Accepted 17 May 2026
Available online 2 June 2026
2213-1388/

channels [4]. High-velocity sites include Saltstraumen (up to 10 m/s), Pentland Firth (>2.5 m/s) [9], and Fall of Warness (up to 4 m/s) [10]. Tidal energy benefits from water's high density, yielding greater energy per unit volume than wind, and predictable cycles enabling up to 20 h/day of generation [11].

At a macro level, the strategic importance of this high predictability is increasingly recognised in contemporary energy planning. Recent techno-economic optimisation studies have demonstrated that integrating tidal energy into regional power systems can significantly enhance grid stability, reduce dispatch-down costs, and accelerate the achievement of net-zero emission targets under deep uncertainty [12].

TECs are broadly classified into tidal range and tidal stream technologies. Tidal stream systems, which extract kinetic energy from currents, are the focus of this work. Among them, Horizontal Axis Turbines (HATs) are the most mature, reaching TRL 8–9 with rated powers between 100 kW and 2 MW, while alternatives such as tidal kites are at TRL 7–8 [4]. HATs can be deployed using different foundation systems [13]:

- Gravity-Based Substructures (GBS) approach employs massive structural foundations that maintain seabed positioning through frictional forces generated by their substantial weight, typically composed of steel or concrete.
- Monopile foundations utilise drilled seabed penetration techniques, analogous to offshore wind installations, and can accommodate dual TEC units mounted on adjustable crossarms that enable operational flexibility for maintenance procedures.
- Floating platform systems utilise seabed-anchored mooring arrangements with heavy anchor systems, supporting dual TEC units positioned beneath the platform to capture energy from elevated water column flows.

Available economic data show substantial variability between tidal energy configurations. For GBS installations, capital expenditure (CapEx) is estimated at 3.65 M€/MW with operational expenditure (OpEx) of 0.18 M€/MW for a 40 MW deployment [14]. Floating platform configurations present lower capital requirements, with industry projections indicating costs of 2.6 M£/MW (CapEx) and 0.20 M£/MW (OpEx) for 10 MW arrays [15]. In contrast, monopile systems demonstrate higher capital requirements; the MeyGen Phase 1C development (73.5 MW capacity) project's investment costs of 6.8 M€/MW, although operational cost data for this configuration remain unavailable [16]. Performance data from UK installations indicate an average capacity factor (CF) of 29.9% for GBS systems [17]. Reported Levelised Cost of Electricity (LCoE) values for tidal stream technologies range between 0.11–0.48 €/kWh, with current estimates of 0.125 €/kWh for floating TEC systems [18] and projections of 0.10 €/kWh by 2030 as deployment scales increase [4].

Commercialisation of tidal energy faces strong competition from mature technologies such as wind and solar; therefore, supportive policy frameworks and long-term deployment programmes remain essential [19]. TECs may play an important role, especially in remote or island communities, where they can enhance energy independence and reduce fossil fuel reliance [20], stimulating economic growth through job creation and reduced energy costs.

The work presented in this paper addresses a clear gap in the existing literature by developing a systematic bottom-up techno-economic modelling framework for the three main HAT configurations, applied to five potential case studies. Specifically, the primary novelty of this work lies in the development of a parametric BuA framework that dynamically scales with specific local bathymetry and hydrodynamic profiles. Unlike traditional top-down methods that rely on macroscopic economic aggregates, this data-driven methodology systematically links foundation-specific structural requirements with site-specific environmental data. This provides a continuous representation of costs across different technologies, rated powers, and installation sites, offering unprecedented transparency for early-stage techno-economic assessments. Tidal resource availability, energy production, and cost metrics are quantitatively evaluated and compared against available literature data.

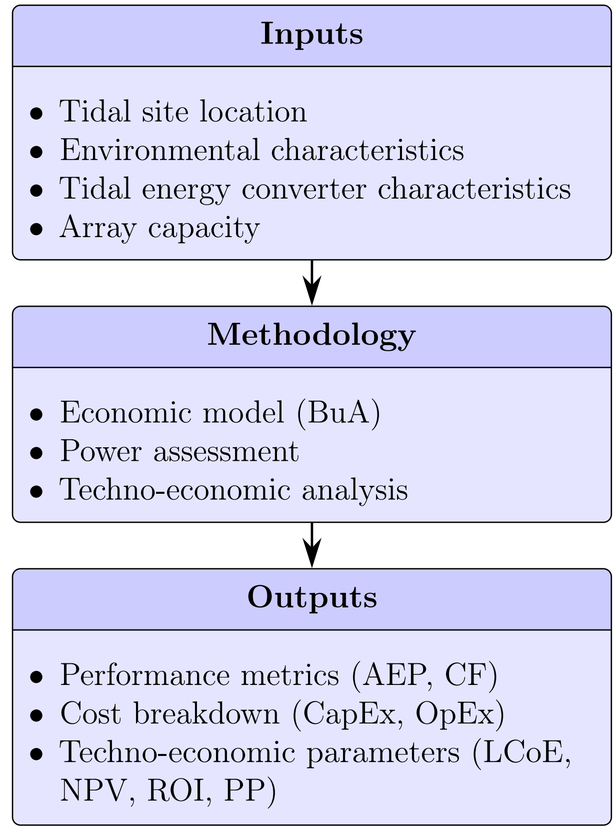

Fig. 1. Workflow of the techno-economic tidal model.

The remainder of the paper is structured as follows: Section "Methods" presents the materials and methods, including study areas, the state of the art of BuA, the tidal resource and power assessment, and the techno-economic assessment; Section "Results and discussion" presents and discusses system performance and competitiveness across sites, including a sensitivity analysis; and Section "Summary and conclusions" provides the summary and main conclusions of the research.

Methods

This study conducts a comprehensive techno-economic feasibility assessment across five distinct locations, evaluating three TEC foundation technologies: Gravity-Based Substructure (GBS), monopile, and floating platform configurations. The analysis integrates site-specific environmental parameters with TEC technical specifications to determine total project costs through the developed cost model. Subsequently, power generation estimates are derived by applying device-specific power curves to local tidal resource characteristics, enabling the calculation of key techno-economic performance indicators. The complete analytical framework, from input parameters to final outputs, is illustrated in Fig. 1.

Study areas

The study focuses on five distinct marine locations selected for their potential in tidal energy exploitation. These sites were chosen based on the availability of tidal current data, existing tidal energy projects, and their diversity in geographical characteristics: the Fall of Warness

(Scotland), Fromveur and Raz Blanchard (France), Punta Pezzo (Italy), and Cozumel (Mexico). The selected sites differ significantly in terms of tidal current velocity, water depth, and proximity to shore, encompassing both nearshore, easily accessible locations and deeper offshore conditions. Fall of Warness is characterised by high tidal velocities (up to 4 m/s [10]), making it an established reference location for device testing and commercial array development. Raz Blanchard exhibits exceptional tidal currents due to the constriction between Alderney Island and Cap de la Hague [21], with depths of approximately 55 m at 11 km from shore. Fromveur provides comparable flow intensity at moderate depths, with particular interest for local off-grid power supply to Ushant Island [22]. Punta Pezzo, in the Strait of Messina, combines strong currents (≈3 m/s) with greater depths (≈100 m), offering logistical advantages due to its coastal proximity [23]. Finally, the Cozumel channel in Mexico represents the shallowest and highly accessible case in this study (≈19 m) [1]. Detailed site descriptions are provided in the Supplementary Material.

These locations were chosen based on accessible tidal data availability, as direct measurements via Acoustic Doppler Current Profilers (ADCPs) present substantial financial constraints [24].

State-of-the-art bottom-up approach

Cost estimation methodologies for technological development can be categorised into two approaches: the Top-down Approach (TdA) and the Bottom-up Approach (BuA). TdA starts from the total project cost and allocates percentages to major system components based on historical data. Although simple to apply, it offers limited insight into how design parameter variations affect component-level costs due to its aggregated structure. Conversely, BuA disaggregates the system into individual subcomponents and technical parameters, enabling the development of detailed cost functions and reducing estimation uncertainty [5]. While TdA provides a high-level perspective, BuA yields more accurate and configuration-specific estimates, although it requires extensive technical data and is less suited to early design stages. Few cost functions specifically designed for TECs are available in the literature. Due to high similarity with wind turbines, many wind turbine component cost functions have been adapted for TEC applications when validity ranges are satisfied. To address this literature gap, this study presents the first comprehensive BuA cost model specifically developed for tidal energy systems, enabling detailed techno-economic comparison of three TEC foundation technologies across five diverse tidal sites and providing technology-specific economic insights through parametric cost functions tailored to marine environments.

Assessment of tidal energy resource

One of the most significant advantages of tidal energy is its high predictability, which follows regular cycles, making precise forecasting of tidal currents and energy generation possible. Due to the high costs of ADCPs, real measurement datasets were not publicly available; instead, only statistical results or a single value were provided. Therefore, four different cases of tidal energy resource assessment were evaluated to present different methodologies in data usage.

1. Model data and bias correction: Tidal velocity data are retrieved from the Global Ocean Physics model provided by the Copernicus Marine Service [25]. The dataset is subsequently corrected using available field measurements, specifically the annual average velocity Uz_{mean} = 1.5 m/s recorded by the ATIR floating platform at a rotor depth of z = 13.9 m [18]. To assess current speeds at the depth of interest, a power law equation is applied, expressed as (1) [26],

$$U(z) = U_{mean} \cdot \left(\frac{h-z}{\beta \cdot h}\right)^{\frac{1}{\alpha}}, \tag{1}$$

where the bed roughness β = 0.4 and power law exponent α = 7 are given parameters from the study that proposed the equation [26], while U_{mean} is the depth-averaged velocity, h is the water depth, and z is the rotor depth. This equation is later used in all case studies.
2. Tidal current time series: in this case, a dataset from the DTOceanPlus project database was retrieved [27], obtained from the HOMERE model developed by Ifremer, using an unstructured grid, and already validated with ADCP measurements [27].
3. Tidal current harmonic analysis: In this case, the harmonic components of the tidal current were provided. Specifically, an ADCP measurement campaign was conducted at the site of interest over a 24-day period. A time-domain harmonic analysis was then carried out, allowing the tidal stream velocity to be estimated as the superposition of sine functions [28].
4. Yearly current frequency analysis: In this case, the use of numerical models such as the Copernicus dataset is not appropriate. This is mainly due to the model's low spatial resolution, which makes it unsuitable for accurately capturing rapid bathymetric variations and the dynamics occurring near the shoreline. Therefore, data for this site were retrieved from the literature. The available data consist of the yearly relative frequency of the depth-averaged current velocity V_{mag}, derived from ADCP measurements [1]. For this specific case, a different, yet comparable, power law velocity profile is used, as it was directly provided together with the velocity data. The vertical velocity distribution is defined as (2),

$$U(z) = U_{mean} \cdot (h-z)^{\frac{1}{b}}, \tag{2}$$

where the power law exponent is $b = 6.14$. The depth-averaged velocity is expressed as

$$V_{mag} = \frac{\int_h^0 U(z)dz}{h} \tag{3}$$

Extractable tidal power

TEC power curves are implemented to estimate the amount of extractable tidal power based on the annual tidal resource dataset, as defined in (4) [7],

$$P = \frac{1}{2}\rho A C_p U^3, \tag{4}$$

where ρ is the water density, set to 1025 $\mathrm{kg/m^3}$, A is the rotor swept area, Cp is the power coefficient, and U is the tidal current speed. Each turbine operates within a specific range of velocity, generating power from the cut-in speed (U_{in}) to the cut-out speed (U_{out}), and delivering rated power (P_{rated}) between the rated speed (U_{rated}) and U_{out}.

Based on the derived tidal power dataset, the annual energy production (AEP) and capacity factor (CF) can be computed [29].

In this analysis, it is assumed that all generated power is transmitted to the onshore substation without accounting for losses through the generator or export cables, and wake effects are neglected. Although omitted in the capacity factor calculations to maintain foundation-independent comparisons, the potential impact of these combined losses on the project's economic viability is rigorously evaluated in the Sensitivity Analysis (Section "Sensitivity analysis").

Techno-economic assessment

This study adopts a techno-economic assessment approach for TECs, in which the overall capital cost is evaluated through a modular cost breakdown based on the primary subsystems of the device. Each subsystem is associated with a specific cost function that reflects the corresponding design parameters, allowing for scalable and flexible cost estimation across different configurations. The main input variables and

Table 1
Main input variables of the BuA-based cost model, with typical ranges of values and assumed values for some parameters.

Parameter	Symbol	Value	Units
Water depth	h	–	/
Distance to the shore	d	–	/
No. of blades	N_{blades}	2–6	/
Rated current	U_{rated}	2–4.5	m/s
Rotor diameter	D	5–24	m
Rated power	P_{rated}	100–2000	kW
No. of turbines per structure	$N_{turb,sub}$	1 or 2	/
No. of structures	N_{sub}	Array dep.	/
Export voltage	V_{export}	11–33	kV
No. of export cables	$N_{cable,exp}$	Array dep.	/
No. of rows for array	N_{row}	Array dep.	/
No. of columns for array	N_{column}	Array dep.	/
Output voltage from generator/array voltage	V_{array}	0.69	kV
Power factor	PF	0.95	/
Gearbox ratio	i	1/98	/
Thrust coefficient	C_T	0.9	/
Ratio of cover and rotor diameter	D_{cover}/D	0.1333	/
Floating platform mass	$M_{platform}$	360	tons
Anchor weight	M_{anchor}	140	tons
Chain diameter	D_{chain}	0.076	m
Steel price for mooring	$P_{steel,mooring}$	0.5	€/kg
Steel price for floating platform	$P_{steel,platform}$	2.5	€/kg
Steel price for GBS	$P_{steel,GBS}$	0.8	€/kg
A36 steel price for monopile	$P_{steel,mono}$	1.2	€/kg
Monopile outer diameter	D_{out}	3.5	m
No mooring lines	$n_{mooring}$	4	/

assumed parameters are listed in Table 1, together with their respective typical ranges of values. A complete list of cost functions related to each TEC component is reported in Tables S1, S2, and S3. Only Development Expenditures (DevEx) were assumed to be 5% of total CapEx without using the BuA [30]. Additionally, nacelle cover cost is considered 21% of nacelle cost (rotor + PTO + yaw system) as derived from the case study in [8].

Some cost functions require input parameters not previously defined, such as the thrust coefficient C_T (used to evaluate the thrust force F_T), low-speed shaft angular velocity ω_{lss}(B.4) and the tip-speed ratio (TSR), set to 4.5 for three-bladed [31] and 6.0 for two-bladed turbines [32].

The assumed values of cost metrics and parameters used in this analysis were retrieved from real tidal energy projects and used as inputs to the corresponding cost functions.

Steel price represents a critical parameter in foundation cost estimation and must be selected according to application-specific requirements. For floating platforms, a steel price of 2.5 €/kg was adopted to reflect the high-quality materials and fabrication requirements typical of offshore structures. The mooring system employs lower-grade steel at 0.5 €/kg, consistent with chain and anchor manufacturing standards. Monopile foundations utilise A36 structural steel, priced at 1.2 €/kg by incorporating an 80% mark-up over base material costs to account for processing and fabrication [33]. GBS structures employ a cost of 0.8 €/kg, reflecting the use of lower-grade steel primarily for ballast purposes, with pricing positioned between raw steel commodity rates [34] and structural steel costs.

Installation costs represent a significant component beyond equipment manufacturing, encompassing turbine substructure, turbine assembly, electrical infrastructure, and mooring system deployment. These costs primarily depend on installation duration and vessel specifications, with rates varying substantially among different vessel types. The general installation cost function for turbines and substructures can be expressed as [35],

$$C_{inst} = \frac{N}{N_{trip}}\left(t_{inst} + 2\frac{d}{V_{vessel}}\right)C_{vessel} = \frac{N}{N_{trip}}\left(t_{inst} + 2\frac{d}{V_{vessel}}\right)\left(C_{rent} + C_{fuel}\right), \quad (5)$$

where N represents the total number of elements to be transported, N_{trip} is the number of elements per trip, d/V_{vessel} is the transit time based on port distance and vessel speed, t_{inst} is the on-site installation time, and C_{vessel} encompasses vessel rental costs, depending on type of vessel and domain of validity of cost variable (see Table S4 [36]), and fuel cost. Environmental factors affecting vessel operations are not modelled due to their complexity and site-specific variability. Additionally, 3 workers are assumed to be on each vessel, with a cost rate of 50 €/h. [5].

The installation time represents the remaining variable needed to complete Eq. (5), and all the installation phases' durations are detailed in Table S5.

Within the installation cost framework, the workers' cost for onshore elements ($N_{elements}$) preparation is evaluated based on a crew of 6 workers, with each element requiring 1 h of preparation time.

For clarity and computational efficiency, the power cable installation cost was estimated following the methodology of [37], assuming one-third of the cable is buried beneath the seabed (282 €/m), and two-thirds is surface-laid (100 €/m).

OpEx comprises all operational and maintenance expenses incurred throughout the plant's operational lifetime, with maintenance activities predominantly executed during suitable weather windows. These costs are conventionally divided into maintenance operations and insurance coverage [8]. The evaluation of maintenance costs presents significant challenges due to their strong dependency on maritime and weather conditions. While many studies quantify OpEx as a fraction of CapEx or per unit of installed capacity, these methodologies cannot adequately reflect the cost variations arising from different system configurations. Although comprehensive modelling frameworks coupled with statistical analysis would provide the most accurate OpEx assessment, the present study prioritises computational simplicity while preserving reasonable cost estimation accuracy. Consequently, maintenance costs are determined through consideration of annual failure rates of key components, associated spare parts expenses (set at 15% of the original component cost), and required repair durations (see Table S6) [38]. Given the absence of specific repair time data for floating and monopile configurations in the available literature, these values were estimated by applying a 30% time reduction compared to the corresponding GBS TEC repair schedules. This reduction was hypothesised based on the operational advantages of floating and monopile systems, which allow for direct surface accessibility, avoiding the complex and time-consuming interventions of a subsea diver or Remotely Operated Vehicle (ROV), typically required for GBS maintenance. Insurance costs are also included in OpEx, assumed to be 1% of CapEx, which aligns closely with findings from the Meygen project [39].

Decommissioning costs (D_c) refer to the expenses associated with the removal of the tidal plant at the end of its operational life. These costs depend on the type of TEC foundation, as different removal techniques and vessel specifications are necessary (see Table S7) [40].

Cost function adjustments

The cost functions and datasets used in this analysis originate from different studies spanning various years, regions, and currencies. To enable consistent economic comparison, all costs were adjusted using the Consumer Price Index (CPI), which accounts for inflation over time and across regions. Economic data were normalised to 2024 values (CPI_{2024}) for each country and expressed in euros for consistency. Each reference cost was scaled according to the corresponding $CPI_{reference,year}$, following the CPI-based adjustment provided in Eq. (B.7) [41], with CPI data summarised in Table S8.

Techno-economic parameters

The evaluation of different TEC configurations requires a robust techno-economic framework. Several financial indicators are employed

Table 2
CapEx and OpEx comparison between model results and real project data.

Component	Model cost [€]	Real cost [€]
Platform	**2,801,801**	**2,876,562**
Structure	900,000	912,787
Mechanical	911,900	1,217,391
Electrical	360,779	327,244
Control	231,538	102,448
Auxiliary	270,808	123,258
Blades	126,777	193,434
Installation	**654,377**	**519,169**
Mooring design	–	10,000
Mooring materials	374,238	200,000
Cable	107,576	106,830
Installation	113,681	83,339
Transport	44,801	100,000
Blade installation	14,080	19,000
Engineering (DevEx)	**181,904**	**158,747**
Design	–	100,909
Construction	–	57,838
Total CapEx	**3,638,083**	**3,554,478**
Maintenance	89,656	–
Insurance	36,377	–
Total OpEx	**126,033**	**96,000**

to estimate plant profitability and feasibility, including the Levelised Cost of Energy (LCoE), Net Present Value (NPV), Return on Investment (ROI), Payback Period (PP), and the amount of avoided CO_2 emissions E_{CO_2}. All techno-economic parameter equations are reported in Appendix "Equations". The discount rate r was assumed to be equal to 5%, and the project lifetime $n = 25$ years [18].

LCoE, NPV, ROI, and PP were calculated according to equations provided in Appendix "Equations", assuming constant annual revenues (R_t) and OpEx over the project lifetime. Electricity revenues were evaluated using an electricity selling price $p_{el} = 207$ €/MWh, consistent with UK tidal energy support schemes [42]. The environmental benefit was quantified through E_{CO_2}, calculated using an emission factor EF of 532 g $CO_{2,eq}$/kWh, representative of electricity production from natural gas [43].

To evaluate model robustness, a multi-variable sensitivity analysis is applied to the most favourable scenario (Fromveur, 32 turbines). This setup represents the highest commercial potential, providing critical insights into the economic viability of large-scale tidal farms.

Results and discussion

This section presents the outcomes of the techno-economic analysis based on the developed BuA model. First, the model is validated against real-world data from the ATIR floating tidal platform to assess its accuracy and consistency with existing project costs. Secondly, the validated model is applied to five selected sites to evaluate and compare the performance and economic feasibility of different TEC configurations under varying environmental conditions.

Cost model validation through ATIR floating TEC

To validate the proposed cost model, a real-world case study was analysed: the ATIR floating tidal platform, developed by Magallanes Renovables and deployed at the EMEC test site in Scotland [44]. Platform characteristics and cost data were collected from technical literature and public sources (see Tables S9 and S10). The export cable was excluded from the model since the ATIR platform was directly connected to EMEC's infrastructure.

Table 2 presents the capital expenditures (CapEx) and operational expenditures (OpEx) estimated by the cost model versus the real costs of the ATIR tidal platform provided by Magallanes Renovables [45].

Most of the cost categories align closely between the model and the real project. Larger deviations are observed in the control and auxiliary components, which include the power converter and wet-mate connectors, respectively. These discrepancies may be present due to outdated cost references or project-specific supply chain conditions. For example, the power converter was reassigned to the control category instead of electrical to better reflect its role and to avoid overestimation.

A significant deviation was found in the mooring material cost. Based on the known mooring system mass and reported project cost, a steel price of approximately 0.26 €/kg would be required to match the real expense. This value is unrealistically low compared to current raw steel prices. Thus, the cost model used 0.5 €/kg, which is consistent with the cost of raw steel [34]. While the total OpEx estimation is reasonably close, the breakdown was not fully available from the developer, so direct comparison of individual components is not possible.

A single case study validation is insufficient to ensure model reliability, necessitating comparison with additional projects of different TEC types. The MeyGen project, comprising four fixed tidal turbines in Scotland's Pentland Firth, represents one of the earliest commercial tidal developments [39]. However, direct cost comparison proves challenging due to the project's pioneering nature. As one of the world's first large-scale tidal arrays, MeyGen encountered significant risks associated with unproven technology, resulting in elevated insurance premiums and contingency costs. The fractured rock seabed and extreme tidal forces required custom engineering solutions for cable stability, further inflating project costs. Additionally, operational expenses were dominated by lease payments and insurance costs, reflecting the high-risk profile of early-stage tidal energy deployment. Consequently, MeyGen's costs substantially exceed both the floating platform case study and the present cost model results, limiting its utility for model validation. Relying solely on the ATIR platform for validation is a recognised limitation due to the current scarcity of commercial data. However, the model's expected reliability for emerging TEC designs and data-scarce sites remains high. By utilising physical and geometric parameters rather than empirical top-down aggregate costs, this bottom-up framework scales effectively. Furthermore, as demonstrated in Section "Sensitivity analysis" , uncertainties in literature-based parameters have a marginal impact on the LCoE compared to the available site-specific energy resource. To systematically address data constraints, future validation efforts will focus on iteratively calibrating the model. As new commercial arrays mature, actual component-level costs and OpEx logs will be statistically aggregated to update the baseline cost functions, thereby reducing overall estimation uncertainties. Beyond its validation scope, the model demonstrates high adaptability to other TEC technologies, alternative sites, and future cost-reduction scenarios, significantly enhancing its practical utility. Its modular structure allows for the seamless integration of emerging devices (e.g., tidal kites), new geographical locations, and projected cost reductions by simply updating the relevant power curves, structural mass equations, and local techno-economic inputs.

Application of the techno-economic model to selected tidal sites

The application of the techno-economic model to selected tidal locations yields various results and techno-economic metrics, which are better listed in Table A.5, and the main insights derived from it are briefly discussed below. Water depth ranges from 19 to 100 metres, with deeper locations such as Punta Pezzo experiencing reduced energy production and increased installation costs for the GBS configuration. Similarly, greater distances from shore, such as the 11 km distance at Raz Blanchard, result in higher power export cable costs, as well as installation and maintenance procedures.

The capacity factor (CF) is computed for each location, with floating and monopile configurations achieving higher values compared to GBS TEC systems, as well as higher annual energy production (AEP). This

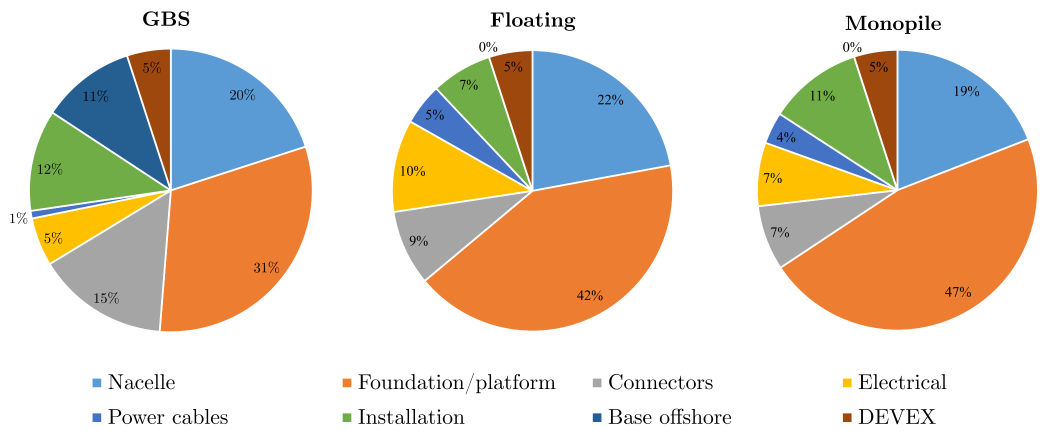

(a) CapEx distribution for 32 TEC array (19.2 MW) in Punta Pezzo.

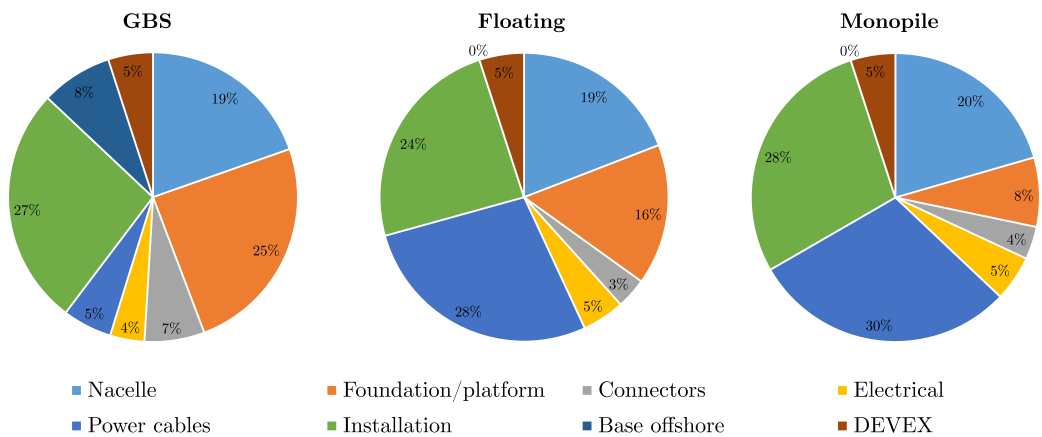

(b) CapEx distribution for 32 TEC array (32 MW) in Raz Blanchard.

Fig. 2. Comparison of CapEx distributions for Punta Pezzo and Raz Blanchard sites.

improved performance results from the higher positioning of the rotor relative to the seabed, which enables the extraction of stronger current velocities and optimises turbine operation. The exception is Cozumel, where the tidal plant operates in shallow water depths. In this case, the GBS rotor must be positioned higher to satisfy the minimum clearance constraint of 6 m between the blade tip and seabed [46]. Additionally, different minimum clearance requirements must be met between the blade tip and sea level: 8 m for GBS configuration and 4.4 m for floating and monopile configurations [47]. Conversely, Punta Pezzo exhibits the lowest CF due to its significant depth, which forces the GBS TEC to operate at considerably lower velocities compared to surface currents, thereby limiting the turbine's operational potential.

Table 3 presents the techno-economic results for the maximum array size considered in this study (32 turbines), which was chosen due to the natural trend of LCoE reduction as the array capacity increases, as later demonstrated in Fig. 4. This corresponds to 32 MW for Fall of Warness, Fromveur, and Raz Blanchard, 19.2 MW for Punta Pezzo, and 3.3 MW for Cozumel. The latter two locations exhibit lower array capacity due to less powerful turbines, as detailed in Table A.5. Cozumel exhibits the lowest OpEx due to its proximity to shore, in contrast to Raz Blanchard, which incurs higher costs due to its distance from land. Most case studies demonstrate profitability, with exceptions being the GBS configuration at Punta Pezzo and all configurations at Cozumel. The unprofitability at Cozumel stems from reduced energy production caused by the less powerful TEC, whose diameter is constrained by shallow water depth, and the site's lower energy resource. In most cases, the monopile TEC achieves the lowest LCoE, except at Punta Pezzo, where high water depth increases foundation costs, making the floating TEC more economically viable. Conversely, GBS consistently shows the lowest profitability across all locations, except at Cozumel, where shallow water depth favours GBS and monopile configurations over floating systems. It should be noted that the floating platform mass and mooring system design are assumed constant in this analysis; in reality, shallow depths and lower currents would reduce both mass and costs.

In Fig. 2, the CapEx distributions for Punta Pezzo and Raz Blanchard are represented for a 32-turbine array, whose tidal sites were selected for high water depth and large distance from shore, respectively. As observed from the pie charts, foundation cost represents the predominant contribution at Punta Pezzo, since the high water depth increases both monopile height and mooring system length, while GBS remains unaffected by this environmental parameter. At Raz Blanchard, power cable cost represents the main contribution to CapEx due to the large distance from shore, except for the GBS configuration, in which the offshore substation allows for a single high-capacity export cable, increasing costs only slightly compared to a nearshore location. Conversely, installation costs are elevated due to the large distance, resulting in longer transit times to reach the tidal plant. Fig. 3 reports the ROI and NPV for these two sites. GBS configurations do not yield a positive return, with the Raz Blanchard GBS TEC achieving only marginal profitability (ROI = 0.004%). In contrast, both floating and monopile configurations show increasing profitability as the array size increases.

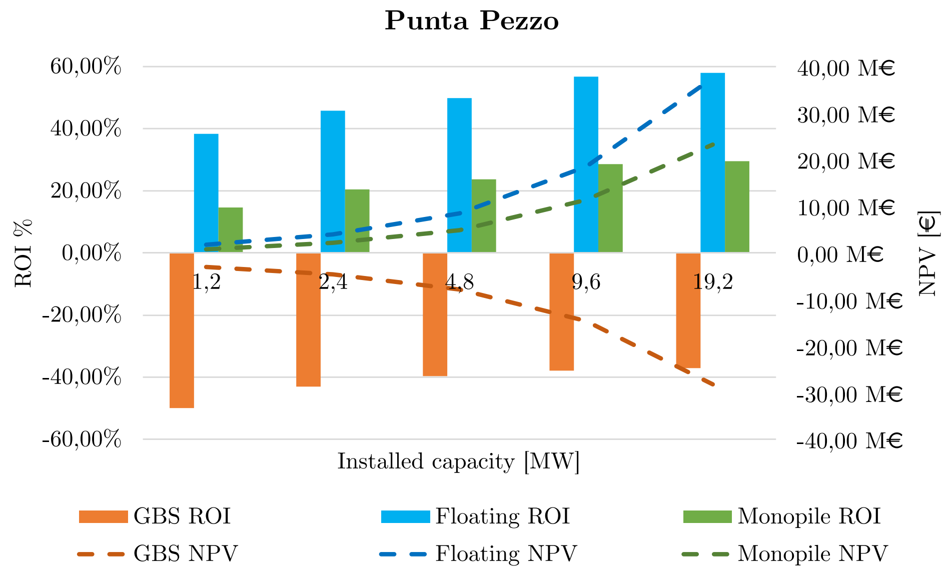

(a) NPV and ROI at different installed capacity and configurations in Punta Pezzo.

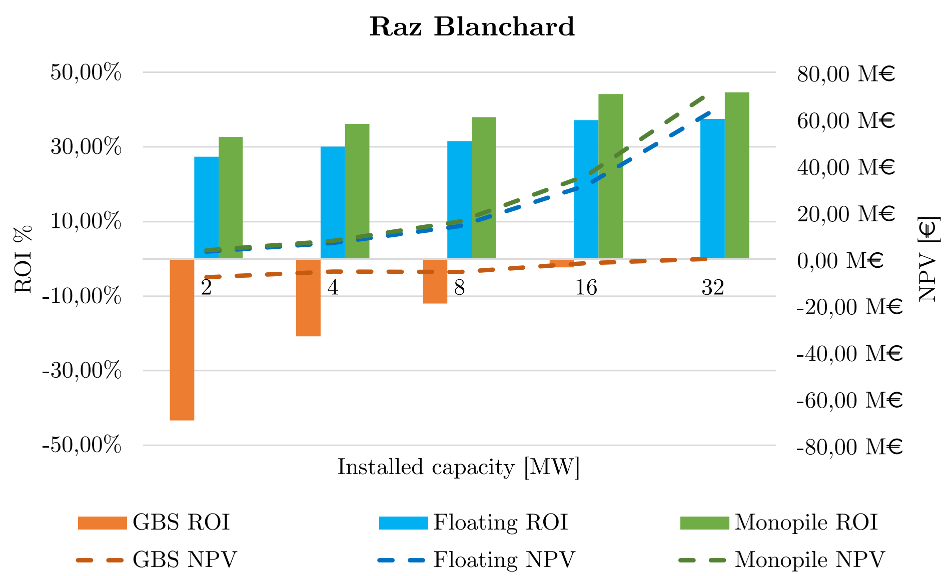

(b) NPV and ROI at different installed capacity and configurations in Raz Blanchard.

Fig. 3. NPV and ROI as a function of Installed Capacity generated by GBS, Floating, and Monopile TECs in Punta Pezzo and Raz Blanchard. Bars and dashed lines represent ROI and NPV values, respectively.

As already observed in Table 3, Fromveur proved to be the most convenient tidal site for a TEC array installation. For this convenient location, the LCoE trend is reported in Fig. 4. The results demonstrate that increasing turbine array capacity leads to a reduction in LCoE values. This trend is most pronounced for GBS TECs, where export cable cost savings become more significant as the turbine number increases. In contrast, floating and monopile TECs exhibit only marginal LCoE reductions because each foundation incorporates its transformer, requiring individual export power cables per foundation. However, this LCoE monotonic decrease may be altered when environmental constraints are explicitly incorporated into the optimisation framework. With their inclusion, the optimal configuration often features fewer turbines than the solution that maximises power output alone. This suggests that the incorporation of site-specific environmental restrictions could result in an optimal array size with a minimum LCoE at intermediate capacities rather than at maximum deployment scales [48].

To place these findings in perspective with other work in the field and benchmark the outcomes of the proposed BuA methodology, the techno-economic results were directly compared against literature estimates derived from top-down approaches and real-world array projections (Table 4). As observed, Fall of Warness and Fromveur achieve CF values close to the UK average (29.9%), while other locations show suboptimal performance due to insufficient resources or mismatched technology. The LCoE targets set by the JRC are only met at Fall of Warness and Fromveur using floating or monopile systems. GBS TECs, representing first-generation devices [17], fail to achieve LCoE below 100 €/MWh due to higher CapEx and OpEx. Literature cost estimates vary significantly and sometimes conflict. The model confirms that floating systems generally incur lower OpEx than GBS, although benchmark values diverge due to high OpEx uncertainty [18]. The modelled CapEx for monopiles differs from the 6.8 M€/MW literature value [16], likely influenced by the high-cost assumptions from the MeyGen Phase 1C project, which in turn was based on elevated costs from the earlier Phase 1A.

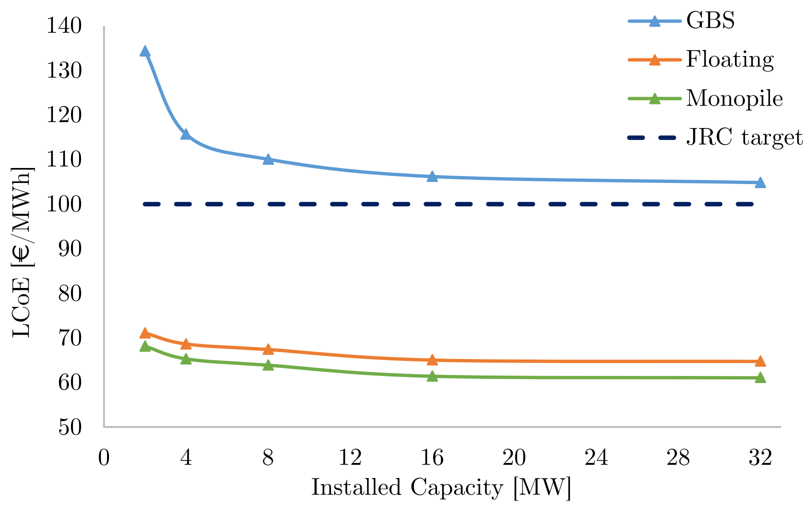

Fig. 4. LCoE trends for GBS, floating, and monopile TEC arrays at Fromveur as a function of installed capacity, with JRC target of 100 €/MWh.

Table 3
Techno-economic assessment results for different configurations.

Parameter	Fall of Warness	Fromveur	Raz Blanchard	Punta Pezzo	Cozumel
GBS configuration					
Installed power [MW]	32	32	32	19.2	3.296
Capacity factor [%]	26.17	31.83	20.24	9.76	12.3
AEP [MWh]	73 444	89 142	56 793	16 427	3554
CapEx [M€]	97.93	100.6	128.9	57.58	24.25
OpEx [M€]	2.02	2.01	2.41	1.11	0.398
LCoE [€/MWh]	124.9	104.9	207.0	328.9	653.1
NPV [M€]	85.01	128.3	0.006	−28.22	−22.35
ROI [%]	65.77	97.33	0.004	–	–
PP [years][a]	10	8	24	–	–
E_{CO_2} [t_{CO_2eq}][b]	39 072	47 423	30 214	8739	1891
Floating configuration					
Installed power [MW]	32	32	32	19.2	3.296
Capacity factor [%]	33.24	39.35	28.49	20.83	11.51
AEP [MWh]	93 066	110 166	79 891	35 040	3325
CapEx [M€]	64.15	74.77	126.6	48.56	30.56
OpEx [M€]	1.60	1.78	2.99	1.09	0.577
LCoE [€/MWh]	66.7	64.8	150.5	131	840.9
NPV [M€]	184.1	220.8	63.64	37.51	−29.7
ROI [%]	210.6	219.4	37.56	57.97	–
PP [years][a]	5	5	13	11	–
E_{CO_2} [t_{CO_2eq}][b]	49 511	58 608	42 502	18 641	1769
Monopile configuration					
Installed power [MW]	32	32	32	19.2	3.296
Capacity factor [%]	33.24	39.35	28.49	20.83	11.51
AEP [MWh]	93 066	110 166	79 891	35 040	3325
CapEx [M€]	47.98	68.24	117.9	57.85	14.78
OpEx [M€]	1.24	1.64	2.81	1.24	0.27
LCoE [€/MWh]	52.6	61.1	143.1	159.8	396.5
NPV [M€]	202.5	226.5	71.99	23.29	−12.45
ROI [%]	293.6	238.6	44.69	29.51	–
PP [years][a]	3	4	12	14	–
E_{CO_2} [t_{CO_2eq}][b]	49 511	58 608	42 502	18 641	1769

[a] PP: Payback Period.
[b] E_{CO_2}: Environmental impact of decarbonisation.

Table 4
Comparison of main techno-economic results and literature values.

TEC	Tidal site	CF [%]	CapEx [M€/MW]	OpEx [M€/MW]	LCoE [€/MWh]
GBS	A	26.17	3.06	0.24	124.87
	B	31.83	3.14	0.20	104.90
	C	20.24	4.03	0.37	206.99
	D	9.76	3.00	0.59	328.88
	E	12.3	24.25	0.98	653.09
	Benchmark [14]	**29.9**	**3.65**	**0.18**	**100** [4]
Floating	A	33.24	2.00	0.15	66.65
	B	39.35	2.34	0.14	64.82
	C	28.49	3.96	0.33	150.48
	D	20.83	2.53	0.27	131.04
	E	11.51	7.36	1.52	840.93
	Benchmark [15]	**29.9**	**3.12**[a]	**0.234**[a]	**100**
Monopile	A	33.24	1.50	0.12	52.59
	B	39.35	2.13	0.13	61.14
	C	28.49	3.69	0.31	143.06
	D	20.83	3.01	0.31	159.83
	E	11.51	9.27	0.71	396.45
	Benchmark [16]	**29.9**	**6.8**	–	**100**

A = Fall of Warness, B = Fromveur, C = Raz Blanchard, D = Punta Pezzo, E = Cozumel.
[a] Currency conversion of 1£ = 1.2€ (January 2025).

Sensitivity analysis

To address uncertainties in key input parameters and evaluate the robustness of the cost model, a sensitivity analysis was conducted on the LCoE. Specifically, this analysis was applied to the maximum array capacity configuration considered in this study (32 turbines) at the most favourable location (Fromveur). The analysis evaluated variations of −20%, −10%, +10%, and +20% across critical drivers. These drivers include the Capacity Factor (CF), discount rate, steel prices, failure rates, and the assumed repairing time reduction for floating and monopile configurations. The resulting percentage variations in LCoE for GBS, floating platforms, and monopile foundations are presented in Fig. 5.

The results indicate that LCoE is primarily governed by the Capacity Factor. A 20% reduction in CF results in an LCoE increase of approximately 25%, while a 20% increase in CF lowers the LCoE by over 15%. In contrast, all other evaluated parameters, such as discount rate, steel prices, and failure rates, exhibit a much lower influence. They drive LCoE variations of less than 10% even at extreme variation

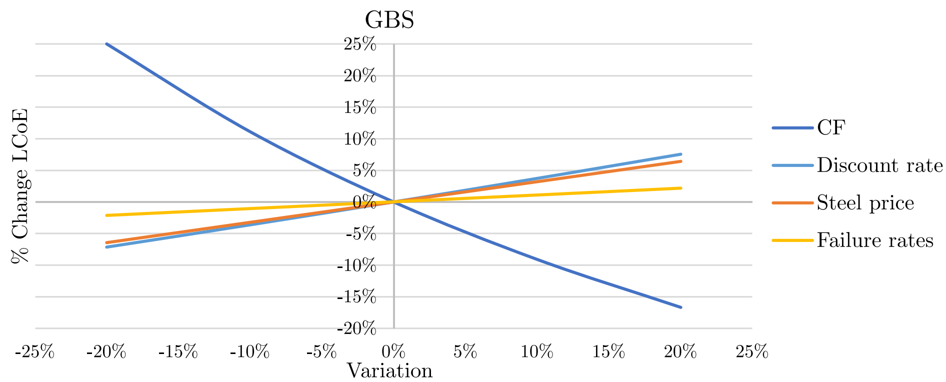

(a) LCoE sensitivity to input parameters for the GBS configuration.

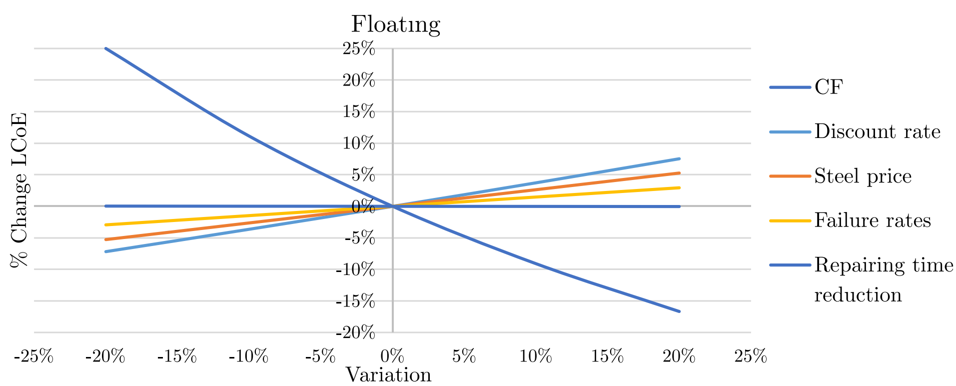

(b) LCoE sensitivity to input parameters for the floating configuration.

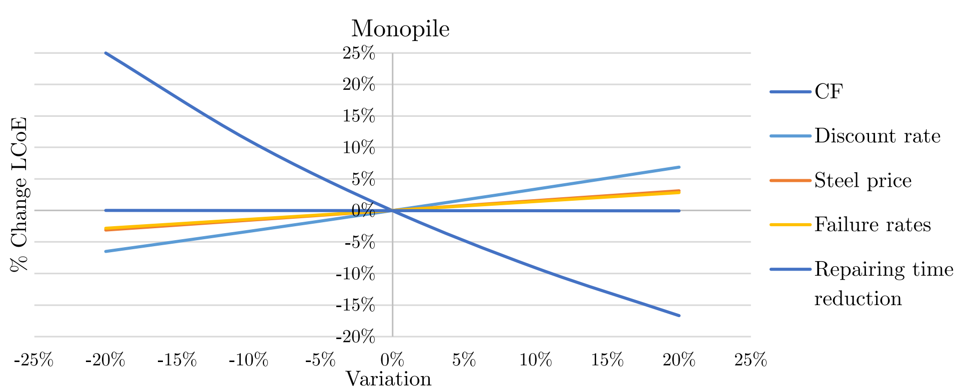

(c) LCoE sensitivity to input parameters for the monopile configuration.

Fig. 5. Sensitivity analysis of the LCoE as a function of percentage variations in key techno-economic parameters (Capacity Factor, Discount rate, Steel prices, Failure rates, and Repairing time reduction).

ranges. Furthermore, the magnitude of these sensitivity trends remains highly consistent across the GBS, floating, and monopile configurations. The only notable exception is the steel price, which exhibits a slightly different sensitivity profile across the technologies due to the distinct baseline material costs assigned to each foundation type, as detailed in Table 1.

Importantly, the sensitivity analysis justifies the OpEx assumptions made in Section "Techno-economic assessment". Due to the scarcity of literature data, a 30% reduction in repair time was assumed for floating and monopile configurations compared to GBS systems. The sensitivity plots demonstrate that LCoE is poorly sensitive to variations in the repairing time reduction, yielding a nearly zero percentage change. Consequently, while precise empirical data for these specific configurations remains limited, the baseline assumptions do not compromise the techno-economic viability and the final LCoE estimates.

The profound sensitivity of LCoE to CF also contextualises some of the highly competitive baseline results, for example, the 52.6 €/MWh for monopiles at Fall of Warness. As stated in the methodology, the current model assumes that all generated power is transmitted without accounting for losses through the generator or export cables, and wake effects are neglected. Because wake interactions and electrical losses are omitted, the effective CF is treated as independent of the TEC array configuration. In a real-world deployment, particularly for large arrays with 32 turbines, wake interactions would incrementally reduce the energy yield of downstream devices. Simulations on a hypothetical large tidal farm (58 turbines) demonstrate that wake losses can induce an error in the active power up to 3%, depending on ambient turbulence [49]. Furthermore, transmission losses would further lower the net electricity delivered to the grid.

Based on the sensitivity findings, if wake effects, electrical losses, and resource estimation uncertainties were to collectively reduce the

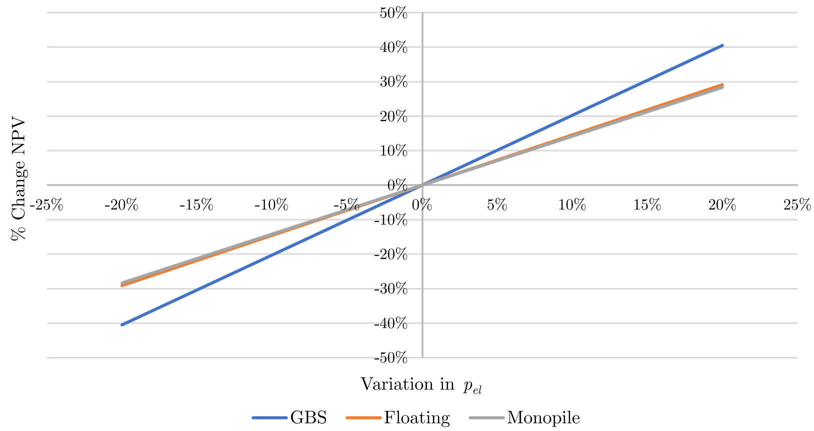

Fig. 6. Sensitivity analysis of the NPV as a function of percentage variations in selling electricity.

effective CF by 10% to 20%, the LCoE would experience a proportional upward shift of 10% to 25%, bringing the estimates closer to conservative literature benchmarks. Furthermore, the inclusion of these losses could slightly influence the comparative advantages between foundation types. For instance, floating systems access higher velocities near the surface and might experience different wake recovery profiles compared to deeper GBS systems. Nonetheless, the overall hierarchy of cost-effectiveness across the tested sites is expected to remain consistent.

Finally, a sensitivity analysis was also applied to the electricity selling price (p_{el}) to evaluate the variability of financial profitability since p_{el} directly impacts the NPV rather than the LCoE. As illustrated in Fig. 6, a 20% fluctuation in p_{el} drives an NPV variation of approximately 30% for floating and monopile configurations, and up to 40% for the GBS system due to its higher investment cost. These results highlight that, in addition to technological optimisation, securing stable government tariffs remains crucial to guarantee the commercial viability of tidal projects.

Environmental and social aspects

The environmental advantages of tidal energy, particularly in terms of CO_2 emission reductions, must be carefully balanced against its social and ecological impacts. Ecologically, differently from floating WECs [50], tidal turbines can affect marine wildlife through collision risks, underwater noise, and electromagnetic fields [51]. Furthermore, turbine arrays can significantly alter regional hydrodynamics by redistributing flow and modifying tidal ranges, which may disrupt sediment and nutrient transport [52]. To account for these factors, future developments of the model can integrate spatial environmental constraints. By including environmental sensitivity maps, the techno-economic model can restrict the available deployment areas. This spatial restriction will directly influence the techno-economic outputs by limiting the maximum number of installable structures and potentially increasing the export cable length to bypass marine protected areas, thereby altering both the optimal array capacity and the final LCoE [53,54]. Conversely, optimisation models can integrate positive externalities by monetising the evaluated avoided CO_2 emissions; assigning an economic value to decarbonisation, for example, through carbon credits, can effectively reduce costs, lower the LCoE, and enhance the technological competitiveness of the project [54]. From a social perspective, successful site selection heavily relies on community engagement to secure public acceptance [55]. Incorporating structured stakeholder consultations into Environmental Impact Assessment (EIA) frameworks is essential to address local concerns and enhance project sustainability. While the current model evaluates DevEx as a flat percentage of CapEx (Section "Techno-economic assessment"), future iterations will extend the bottom-up approach to formulate dedicated cost functions for permitting, EIA procedures, and community engagement activities. This refinement will accurately quantify the financial impact of regulatory compliance and social acceptance. Ultimately, coupling these metrics with tangible socioeconomic benefits, such as local electricity supply, will be crucial to secure community support and align deployments with national energy goals [56].

Summary and conclusions

This study presented a novel, fully parametric bottom-up (BuA) techno-economic framework for evaluating three key tidal energy converter (TEC) configurations: Gravity-Based Substructures (GBS), monopile foundations, and floating platforms, across five distinct coastal sites. A major achievement of this methodology is its ability to overcome the limitations of traditional top-down approaches by employing detailed cost functions derived from physical, geometric, and industry data. This provides unprecedented transparency in identifying the primary cost drivers for different foundation-site pairings.

The analysis showed that monopile and floating TECs generally achieve better performance in terms of capacity factor and Levelised Cost of Energy (LCoE), especially at sites such as Fall of Warness and Fromveur, where LCoE values dropped below 65 €/MWh. These results meet the European Commission's cost targets for tidal energy. Floating platforms proved most suitable for deep-water locations like Punta Pezzo, while monopile configurations were more cost-effective in shallower waters. GBS systems, although less competitive overall, showed relative advantages in shallow, nearshore sites like Cozumel. The model was successfully validated against the real-world ATIR floating platform, showing good agreement in terms of capital and operational costs, thus reinforcing the robustness of the proposed methodology.

Regarding future research perspectives, the modular architecture of this bottom-up framework lays the groundwork for several critical advancements. First, future iterations will quantitatively integrate spatial environmental constraints directly into the optimisation loop, which will dynamically affect array sizing and cable routing. Second, the model will be expanded to formulate dedicated, parametric cost functions for Development Expenditures (DevEx), thereby translating social acceptance into the cost-optimisation process. Finally, future work will focus on multi-technology validation, cross-referencing model outputs with operational data from maturing commercial arrays to continuously calibrate probabilistic failure models and capture OpEx uncertainties in extreme marine environments.

Overall, the methodology developed here represents a highly adaptable and scalable tool to support decision-making in early-stage design and site selection. It contributes to advancing the economic viability of marine renewables by providing realistic, component-based cost assessments tailored to environmental and technological variability.

Table A.5
Summary of main characteristics of selected tidal sites and tidal turbines.

	Parameter	Fall of Warness	Fromveur	Raz Blanchard	Punta Pezzo	Cozumel
Site location	Latitude	59.14°	48.44°	49.76°	38.23°	20.51°
	Longitude	−2.82°	−5.03°	−2.01°	15.63°	−86.95°
Environmental parameters	Water depth [m]	49	51.3	55	100	19.1
	Distance from shore [m]	1600	2500	11 100	600	19.1
Tidal turbine characteristics	Turbine name	Orbital O2	Seagen S-2 MW	Seagen S-2 MW	Seagen S-1.2 MW	Tocardo T2
	Foundation	Floating	Monopile	Monopile	Monopile	Tidal range
	Rotor diameter [m]	20	20	20	16	9.9
	Rated power [kW]	1000	1000	1000	600	103
	Rated current [m/s]	2.65	2.5	2.5	2.35	2
	Cut-in velocity [m/s]	1	1	1	0.7	0.4
	Cut-out velocity [m/s]	4	4	4	4	2.6

CRediT authorship contribution statement

M. Petri: Writing – review & editing, Writing – original draft, Visualization, Validation, Supervision, Software, Resources, Project administration, Methodology, Investigation, Formal analysis, Data curation, Conceptualization. **E. Gorr-Pozzi:** Writing – review & editing, Writing – original draft, Visualization, Validation, Supervision, Software, Resources, Project administration, Methodology, Investigation, Formal analysis, Data curation, Conceptualization. **M. Corrales-González:** Writing – review & editing, Visualization, Validation, Supervision, Software, Resources, Methodology, Investigation, Formal analysis, Data curation. **G. Giorgi:** Writing – review & editing, Supervision, Project administration, Investigation, Funding acquisition, Conceptualization.

Funding

This research was funded by the European Union – NextGenerationEU Award Number: Project code PE0000021, Concession Decree No. 1561 of 11.10.2022, adopted by Ministero dell'Universitá e della Ricerca (MUR), Italy, CUP, Italy E13C22001890001, Project title "Network 4 Energy Sustainable Transition – NEST". Additionally, this project has received funding from the European Union's Horizon Europe Research and Innovation Programme of Blue Energy Offshore Installation Accelerator (Blue-X) under Grant Agreement No 101131527.

Declaration of competing interest

The authors declare that they have no known competing financial interests or personal relationships that could have appeared to influence the work reported in this paper.

Acknowledgements

We are grateful to the European Union's Horizon Europe Research and Innovation Programme of Blue Energy Offshore Installation Accelerator (Blue-X) for the funding Grant Agreement No 101131527, the Marine Offshore Renewable Energy Lab (MOREnergy) Lab-DIMEAS (Politecnico di Torino) for supporting this research. All authors have read and agreed to the published version of the manuscript.

Appendix A. Data of selected tidal sites and turbines

See Table A.5.

Appendix B. Equations

Here's a list of equations of variables/techno-economic parameters involved in this study [14,29,37,43,57,58,58,59].

$$AEP = P_{yearly\,mean} \cdot 8760\,, \tag{B.1}$$

$$CF = \frac{P_{yearly\,mean}}{P_{rated}} \tag{B.2}$$

$$F_T = \frac{1}{2}\rho A C_T U^2\,, \tag{B.3}$$

$$\omega_{lss} = \frac{U \cdot TSR}{D/2} \tag{B.4}$$

$$N_{elements} = N_{blades} + N_{foundation} + N_{chain\ lines} + N_{anchors} + N_{shackles} \tag{B.5}$$

$$C_{cable,inst} = 100 \cdot \frac{2}{3} \cdot L + 282 \cdot \frac{1}{3} \cdot L\,, \tag{B.6}$$

$$COST_{2024} = COST_{reference,year} \cdot \frac{CPI_{2024}}{CPI_{reference,year}}, \tag{B.7}$$

$$LCoE = \frac{CapEx + \sum_{t=1}^{n} \frac{OpEx_t}{(1+r)^t} + \frac{D_c}{(1+r)^n}}{\sum_{t=1}^{n} \frac{AEP_t}{(1+r)^t}}\,, \tag{B.8}$$

$$NPV = -CapEx + \sum_{t=1}^{n} \frac{R_t - OpEx_t}{(1+r)^t} + \frac{D_c}{(1+r)^n}\,, \tag{B.9}$$

$$R_t = AEP_t \cdot p_{el}\,, \tag{B.10}$$

$$ROI\ [\%] = \frac{NPV}{C_{tot}}\,, \tag{B.11}$$

$$C_{tot} = CapEx + \sum_{t=1}^{n} \frac{OpEx_t}{(1+r)^t} + \frac{D_c}{(1+r)^n}\,, \tag{B.12}$$

$$PP = \frac{\ln\left(\frac{R-OpEx}{R-OpEx-r\cdot CapEx}\right)}{\ln(1+r)}\,, \tag{B.13}$$

$$E_{CO_2} = EF \cdot AEP\,, \tag{B.14}$$

Appendix C. Supplementary data

Supplementary material related to this article can be found online at https://doi.org/10.1016/j.seta.2026.105052.

Data availability

Data will be made available on request.

References

[1] Alcérreca-Huerta JC, Encarnacion JI, Ordoñez-Sánchez S, Callejas-Jiménez M, Gallegos Diez Barroso G, Allmark M, Mariño-Tapia I, Silva Casarín R, O'Doherty T, Johnstone C, Carrillo L. Energy yield assessment from ocean currents in the insular shelf of Cozumel Island. J Mar Sci Eng 2019;7(5):147. http://dx.doi.org/10.3390/jmse7050147.

[2] Russell A, Firestone J, Bidwell D, Gardner M. Place meaning and consistency with offshore wind: An island and coastal tale. Renew Sustain Energy Rev 2020;132. http://dx.doi.org/10.1016/j.rser.2020.110044.

[3] Frost C. Quantifying the benefits of tidal stream energy to the wider UK energy system. Tech. rep., Offshore Renewable Energy Catapult; 2022, URL https://ore.catapult.org.uk/analysisinsight/quantifying-the-benefits-of-tidal-stream-energy-to-the-wider-uk-energy-system.

[4] Tapoglou E, Mc Govern L, Georgakaki A, Mountraki A, Letout S, Ince E, Gea Bermudez J, Schmitz A, Grabowska M. Clean energy technology observatory: ocean energy in the european union - 2024 status report on technology development, trends, value chains and markets. Tech. rep., Joint Research Centre; 2024, http://dx.doi.org/10.2760/1244922.

[5] Giglio E, Petracca E, Paduano B, Moscoloni C, Giorgi G, Sirigu SA. Estimating the cost of wave energy converters at an early design stage: A bottom-up approach. Sustainability 2023;15(8). http://dx.doi.org/10.3390/su15086756.

[6] Konuk E-B, Centeno-Telleria M, Zarketa-Astigarraga A, Aizpurua J-I, Giorgi G, Bracco G, Penalba M. On the definition of a comprehensive technology-informed accessibility metric for offshore renewable energy site selection. J Mar Sci Eng 2023;11(9). http://dx.doi.org/10.3390/jmse11091702.

[7] Bajpai U, Singal SK. Techno-economic assessment of hydrokinetic technology: A case study. Energy Sustain Dev 2025;89. http://dx.doi.org/10.1016/j.esd.2025.101872.

[8] Segura E, Morales R, Somolinos JA. Cost assessment methodology and economic viability of tidal energy projects. Energies 2017;10(11). http://dx.doi.org/10.3390/en10111806.

[9] Tan T, Vengatesan V. Enhancing wave resource assessment of high energy sites through wave-current interaction modelling. 2025, http://dx.doi.org/10.2139/ssrn.5281396, SSRN Preprint.

[10] Evans L, Ashton I, Sellar BG. Impact on energy yield of varying turbine designs under conditions of misalignment to the current flow. Energies 2023;16(9). http://dx.doi.org/10.3390/en16093923.

[11] Magagna D, MacGillivray A, Jeffrey H, Hanmer C, Raventos A, Badcock-Broe A, Tzimas E. Wave and tidal energy strategic technology agenda. Tech. rep., SI Ocean; 2014, URL https://www.policyandinnovationedinburgh.org/wave-and-tidal-energy-strategic-technology-agenda.html.

[12] Sabzpoosh Saravi V, Liu X, Frost C. Power system planning under deep uncertainty: Integrating tidal energy for net-zero Northern Ireland. Appl Energy 2026;404:127140. http://dx.doi.org/10.1016/j.apenergy.2025.127140.

[13] Segura E, Morales R, Somolinos J, López A. Techno-economic challenges of tidal energy conversion systems: Current status and trends. Renew Sustain Energy Rev 2017;77:536–50. http://dx.doi.org/10.1016/j.rser.2017.04.054.

[14] O'Connell R, Kamidelivand M, Polydoros I, Wright C, Bonar P, Williams AJ, Murphy J. The integration of tools for the techno-economic evaluation of fixed and floating tidal energy deployment in the irish sea. Energies 2023;16(22). http://dx.doi.org/10.3390/en16227526.

[15] OffshoreWIND. Scotrenewables secures GBP 7.6 million for tidal energy project (UK). 2012, URL https://www.offshorewind.biz/2012/12/14/scotrenewables-secures-gbp-7-6-million-for-tidal-energy-project-uk/. [Accessed 13 January 2025].

[16] Santhakumar S, Meerman H, Faaij A. Future costs of key emerging offshore renewable energy technologies. Renew Energy 2024;222:119875. http://dx.doi.org/10.1016/j.renene.2023.119875.

[17] Iyer A, Couch S, Harrison G, Wallace A. Variability and phasing of tidal current energy around the United Kingdom. Renew Energy 2013;51:343–57. http://dx.doi.org/10.1016/j.renene.2012.09.017.

[18] Bianchi M, Arnal A, Astorkiza-Andres M, Clavell-Diaz J, Marques A, Isasa-Sarralde M. Life cycle and economic assessment of tidal energy farms in early design phases: Application to a second-generation tidal device. Heliyon 2024;10(12). http://dx.doi.org/10.1016/j.heliyon.2024.e32515.

[19] Rose D. 2024 state of the science report - chapter 7: Rducation and outreach around environmental effects of marine renewable energy. Tech. rep., Pacific Northwest National Laboratory (PNNL); 2024, URL https://tethys.pnnl.gov/publications/2024-state-science-report-chapter-7-education-outreach-around-environmental-effects.

[20] Vargiu A, Novo R, Moscoloni C, Giglio E, Giorgi G, Mattiazzo G. An energy cost assessment of future energy scenarios: A case study on San Pietro Island. Energies 2022;15(13). http://dx.doi.org/10.3390/en15134535.

[21] Campbell R, Martinez A, Letetrel C, Rio A. Methodology for estimating the French tidal current energy resource. Int J Mar Energy 2017;19:256–71. http://dx.doi.org/10.1016/j.ijome.2017.07.011.

[22] Ocean Energy Europe. Sabella. 2025, URL https://www.oceanenergy-europe.eu/annual/sabella. [Accessed 28 September 2025].

[23] Barbarelli S, Florio G, Amelio M, Scornaienchi N, Cutrupi A, Lo Zupone G. Design procedure of an innovative turbine with rotors rotating in opposite directions for the exploitation of the tidal currents. Energy 2014;77:254–64. http://dx.doi.org/10.1016/j.energy.2014.08.044.

[24] Togneri M, Lewis M, Neill S, Masters I. Comparison of ADCP observations and 3D model simulations of turbulence at a tidal energy site. Renew Energy 2017;114:273–82. http://dx.doi.org/10.1016/j.renene.2017.03.061.

[25] CMDS-EU. Copernicus marine data store. 2024, http://dx.doi.org/10.48670/moi-00016, URL https://data.marine.copernicus.eu/products. [Accessed 22 November 2024].

[26] Lewis M, Neill S, Robins P, Hashemi M, Ward S. Characteristics of the velocity profile at tidal-stream energy sites. Renew Energy 2017;114:258–72. http://dx.doi.org/10.1016/j.renene.2017.03.096.

[27] European Climate, Infrastructure and Environment Executive Agency (CINEA). DtOceanPlus—Design tools for ocean energy systems innovation. 2021, URL https://cinea.ec.europa.eu/featured-projects/dtoceanplus_en. [Accessed 28 September 2025].

[28] Balestrino F, Coiro D, Giannini G, Giudice D, Troise G. Resource assessment for the GEMSTAR tidal current energy harvester deployment in the strait of Messina. In: 13th European wave and tidal energy conference, Naples, Italy. 2019, p. 10, URL https://www.researchgate.net/publication/337275969_Resource_assessment_for_the_GEMSTAR_tidal_current_energy_harvester_deployment_in_the_strait_of_Messina.

[29] Abed K, El-Mallah A. Capacity factor of wind turbines. Energy 1997;22(5):487–91. http://dx.doi.org/10.1016/S0360-5442(96)00146-6.

[30] Núñez Rivas LR, López Piñeiro A, Somolinos Sánchez JA, Novoa Rojas EM, Carneros Lozano A. Comparative analysis of life cycle costs between the 2nd generation TEC GESMAY and a 1st generation TEC. In: 11th European wave and tidal energy conference, nantes, France. 2015, p. 10, URL https://oa.upm.es/38538/.

[31] Fernandez-Rodriguez E, Stallard T, Stansby P. Experimental study of extreme thrust on a tidal stream rotor due to turbulent flow and with opposing waves. J Fluids Struct 2014;51:354–61. http://dx.doi.org/10.1016/j.jfluidstructs.2014.09.012.

[32] Finnegan W, Fagan E, Flanagan T, Doyle A, Goggins J. Operational fatigue loading on tidal turbine blades using computational fluid dynamics. Renew Energy 2020;152:430–40. http://dx.doi.org/10.1016/j.renene.2019.12.154.

[33] MetalMiner. Steel prices & dynamic steel price forecasting for 2025. 2025, URL https://agmetalminer.com/metal-prices/carbon-steel/. [Accessed 17 January 2025].

[34] FocusEconomics. Steel (USA) prices. 2025, URL https://www.focus-economics.com/commodities/base-metals/steel-usa/. [Accessed 02 January 2025].

[35] Martinez A, Iglesias G. Multi-parameter analysis and mapping of the levelised cost of energy from floating offshore wind in the Mediterranean Sea. Energy Convers Manage 2021;243. http://dx.doi.org/10.1016/j.enconman.2021.114416.

[36] Correia da Fonseca F, Bento do Amaral L, Rentschler M, Arede F, Chainho P, Yang Y, Noble D, Petrov A, Nava V, Germain N, Lariviere-Gillet N, Henderson J, Hudson B. DTOceanPlus deliverable d5.7 - logistics and marine operations tools -alpha version. Tech. rep., WavEC - Offshore Renewables; 2020, http://dx.doi.org/10.13140/RG.2.2.34806.61765.

[37] Tétu A, Chozas JF, Kofoed JP. Liftwec development of a new class of wave energy converter based on hydrodynamic lift forces deliverable d8.1: cost database. Tech. rep., Aalborg University; 2020, URL https://liftwec.com/d8-1-cost-database/.

[38] Kamidelivand M, Deeney P, McAuliffe FD, Leyne K, Togneri M, Murphy J. Scenario analysis of cost-effectiveness of maintenance strategies for fixed tidal stream turbines in the Atlantic Ocean. J Mar Sci Eng 2023;11. http://dx.doi.org/10.3390/jmse11051046.

[39] Black&Veatch. Lessons learnt from Meygen phase 1a: Final summary report. Tech. rep., Department for Business Energy and Industrial Strategy (BEIS); 2020, URL https://tethys-engineering.pnnl.gov/publications/lessons-learnt-design-installation-initial-operations-phases-6mw-4-turbine-tidal-array.

[40] ARUP. Review of approaches and cost of decommissioning small scale offshore renewable energy developments. Tech. rep., Ove Arup & Partners Ltd; 2018, URL https://consult.gov.scot/marine-scotland/offshore-renewables-decommissioning-guidance/supporting_documents/MSLOT%20small%20scale%20OREI%20decommissioning%20%20Final%20issue.pdf.

[41] US Bureau of Labor Statistics. How to use the consumer price index for escalation. 2023, URL https://www.bls.gov/cpi/factsheets/escalation.htm. [Accessed 13 January 2025].

[42] Maksumic Z. UK awards six tidal stream projects with contracts for difference in allocation round 6. 2024, URL https://www.offshore-energy.biz/uk-awards-six-tidal-stream-projects-with-contracts-for-difference-in-allocation-round-6/. [Accessed 14 January 2025].

[43] Corrales-Gonzalez M, Lavidas G, Lira-Loarca A, Besio G. Wave energy assessment and wave converter applicability at the Pacific coast of Central America. Front Energy Res 2024;12. http://dx.doi.org/10.3389/fenrg.2024.1454275.

[44] Renovables M. Magallanes Renovables. URL https://www.magallanesrenovables.com/.

[45] Magallanes Renovables. Magallanes renovables: Business deck. 2020, URL https://maritime-forum.ec.europa.eu/document/download/85b06a7e-2ba4-43f4-938d-8f6bca1336c2_en?filename=magallanes_renovables_-_investor_deck_.blueinvest.pdf&prefLang=mt. [Accessed 14 January 2025].
[46] MeyGen Ltd. MeyGen tidal energy project phase 1 environmental statement. Tech. rep., MeyGen Ltd; 2012, URL https://tethys.pnnl.gov/sites/default/files/publications/MeyGen-2012-ES.pdf.
[47] European Marine Energy Centre (EMEC). Magallanes ATIR project information summary. Tech. rep., European Marine Energy Centre Ltd (EMEC); 2021, URL https://marine.gov.scot/sites/default/files/project_information_summary_12.pdf.
[48] González-Gorbeña E, Pacheco A, Plomaritis TA, Ferreira Ó, Sequeira C. Estimating the optimum size of a tidal array at a multi-inlet system considering environmental and performance constraints. Appl Energy 2018;232:292–311. http://dx.doi.org/10.1016/j.apenergy.2018.09.204.
[49] Brutto OAL, Barakat MR, Guillou SS, Thiébot J, Gualous H. Influence of the wake effect on electrical dynamics of commercial tidal farms: Application to the Alderney race (France). IEEE Trans Sustain Energy 2018;9(1):321–32. http://dx.doi.org/10.1109/TSTE.2017.2731839.
[50] Battisti B, Giorgi G, Fernandez GV. Balancing power production and coastal protection: A bi-objective analysis of wave energy converters. Renew Energy 2024;220. http://dx.doi.org/10.1016/j.renene.2023.119702.
[51] Copping AE, Hemery LG, Overhus DM, Garavelli L, Freeman MC, Whiting JM, Gorton AM, Farr HK, Rose DJ, Tugade LG. Potential environmental effects of marine renewable energy development—The state of the science. J Mar Sci Eng 2020;8(11). http://dx.doi.org/10.3390/jmse8110879.
[52] Huang Z, Dai P, Zhang J. Joint development of tidal current energy in multi-channels surrounding Xiushan Island, China. Energy 2026;347:140327. http://dx.doi.org/10.1016/j.energy.2026.140327.
[53] Olivia L. Artificial reef effect in relation to offshore renewable energy conversion: state of the art. Sci World J 2012. http://dx.doi.org/10.1100/2012/386713.
[54] Wen Y, Low YM. Assessment of tidal stream energy and decarbonization potential by high-resolution simulations: A case study for Singapore. Energy Convers Manage 2026;348:120771. http://dx.doi.org/10.1016/j.enconman.2025.120771.
[55] Howell A, Drake C. Scoping study on socio-economic impacts of tidal energy development in Nova Scotia: a research synthesis & priorities for future action. Tech. rep., Nova Scotia Department of Energy & Offshore Energy Environmental Research Association; 2012, URL https://oera.ca/research/scoping-study-socio-economic-impacts-tidal-energy-development-nova-scotia-research.
[56] Wijesuriya BPK, Afrouzi HN, Liew SC. Evaluating the potential of tidal energy in Malaysia: Economic and environmental benefits of the Kuching barrage project. Energy Sustain Dev 2026;92:101969. http://dx.doi.org/10.1016/j.esd.2026.101969.
[57] Martin-Short R, Hill J, Kramer S, Avdis A, Allison P, Piggott M. Tidal resource extraction in the Pentland Firth, UK: Potential impacts on flow regime and sediment transport in the inner sound of Stroma. Renew Energy 2015;76:596–607. http://dx.doi.org/10.1016/j.renene.2014.11.079.
[58] Nabil MH, Barua J, Eiva URJ, Ullah MA, Chowdhury TA, Siddiquee SMS, Alam ME, Das R. Techno-economic analysis of commercial-scale 15 MW on-grid ground solar PV systems in Bakalia: A feasibility study proposed for BPDB. Energy Nexus 2024;14. http://dx.doi.org/10.1016/j.nexus.2024.100286.
[59] Bhandari SB. Discounted payback period: Some extensions. In: Proceedings of the ASBBS annual conference. vol. 16, Las Vegas; 2009.